Supplement of Biogeosciences, 12, 6869–6880, 2015
http://www.biogeosciences.net/12/6869/2015/
doi:10.5194/bg-12-6869-2015-supplement

Biogeosciences Open Access EGU

Supplement of

pH up-regulation as a potential mechanism for the cold-water coral *Lophelia pertusa* to sustain growth in aragonite undersaturated conditions

M. Wall et al.

Correspondence to: M. Wall (mwall@geomar.de)

Material and Method:

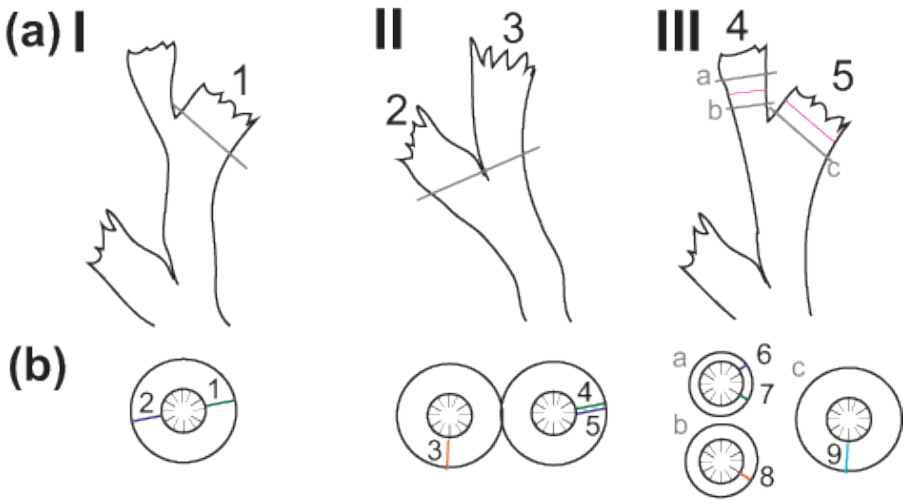

Figure S1: Schematic representation of (a) colonies (I-III) and polyps (1-5) analysed for boron isotopic composition. Indicated in (a) are the cuts (in grey) through the different polyps. (b) the location of the performed SIMS transects (1-9) on the different polyps. The line in colony III, polyp 4 represents the staining line. Cut a is performed above the staining line and cut b and c below.

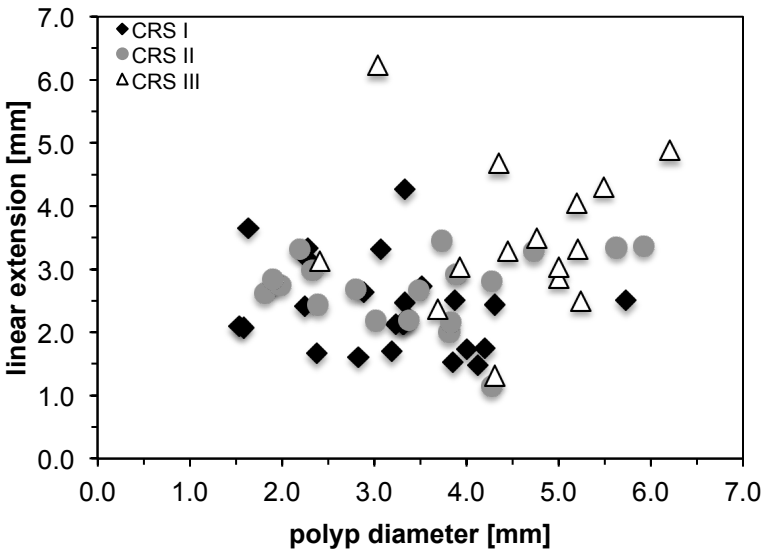

Figure S2: Polyp diameter as a function of linear extension rate for the different experimental treatments CRSI, CRSII and CRSIII. No relationship was observed between polyp diameter and growth as linear extension rate (r^2 = 0.04, n = 60).

Results:

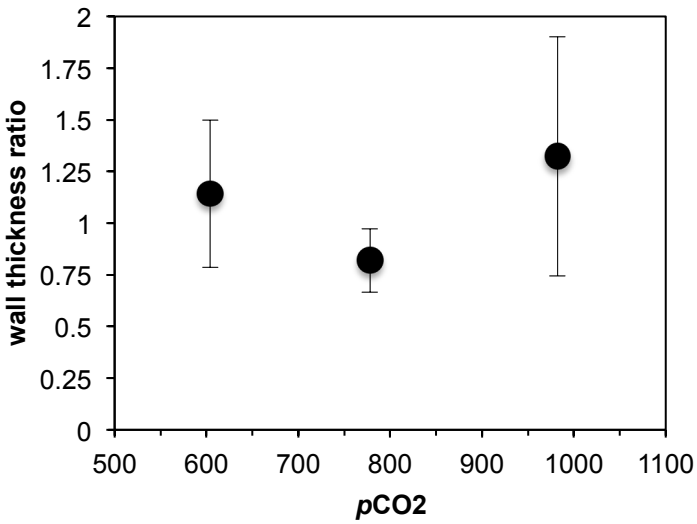

Figure S3: Wall thickness displayed as ratio of thickness below and above the alizarin staining line for the different pCO_2 treatments (mean ± SD; n = 5-7)

Table S1: Average $\delta^{11}B$ values from all transects (transect numbers (#) are indicatd in respective figures in the manuscript and supplements) for the different skeletal regions (primary and secondary) were Raman revealed location of the skeletal regions and averaged for natural (Nat) and treatment samples (CRSIII). These values were converted into internal calcifying fluid pH (pH_{cf}). All values are mean and standard deviation in brackets.

Transect	**#1**	**#2**	**#3**	**#4**	**#5**	**#6**	**#7**	**#8**	**#9**	**⌀ nat**	**⌀ CRSIII**
$\delta^{11}B$ primary skeleton	22.55 (1.78)	22.87 (2.02)	21.37	22.22 (0.98)	22.96	24.81 (1.39)	24.73 (1.56)	23.70 (2.02)	22.79 (1.59)	**22.48 (1.58)**	**24.52 (1.21)**
$\delta^{11}B$ secondary skeleton	29.17 (2.69)	28.09 (2.30)	28.06 (1.83)	28.70 (4.88)	28.58 (1.87)		27.10		27.22 (1.74)	**28.73 (4.73)**	**27.80 (1.94)**
pH_{cf} primary skeleton	8.59 (0.12)	8.62 (0.14)	8.51	8.58 (0.07)	8.63	8.76 (0.09)	8.74 (0.06)	8.69 (0.14)	8.61 (0.11)	**8.58 (0.11)**	**8.74 (0.08)**
pH_{cf} secondary skeleton	9.03 (0.18)	8.99 (0.15)	8.95 (0.12)	9.03 (0.37)	8.99 (0.13)		8.92		8.90 (0.11)	**9.01 (0.15)**	**8.95 (0.13)**

Additional $\delta^{11}B$ transects display the variation of $\delta^{11}B$ with the coral growth growth stage, i.e. primary to secondary skeleton formation towards the outer rim and the influence of Alizarin staining.

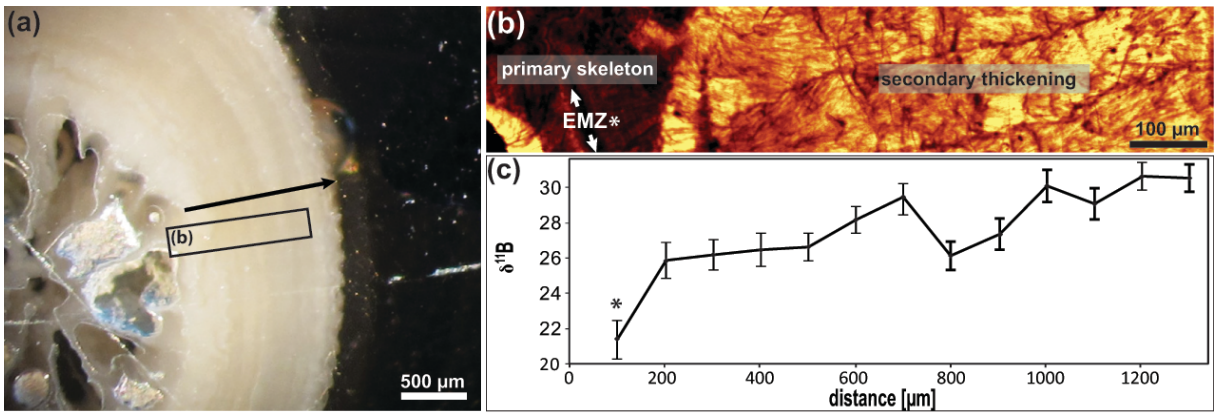

Figure S4: Old branch of *Lophelia pertusa* cut in transversal plane and prepared for Raman mapping and SIMS analysis. (a) Microscopic image contains the location of the Raman map and the SIMS transects. (b) Raman map of the intensity distribution of the main aragonite peak (symmetric stretch, 1085 cm^{-1}) reveals the early mineralization zone (EMZ), the primary skeleton and the area of secondary thickening. Asterisks mark EMZ in the primary skeleton. c) $\delta^{11}B$ measured from inside to the outer coral skeletal rim (transect #3)

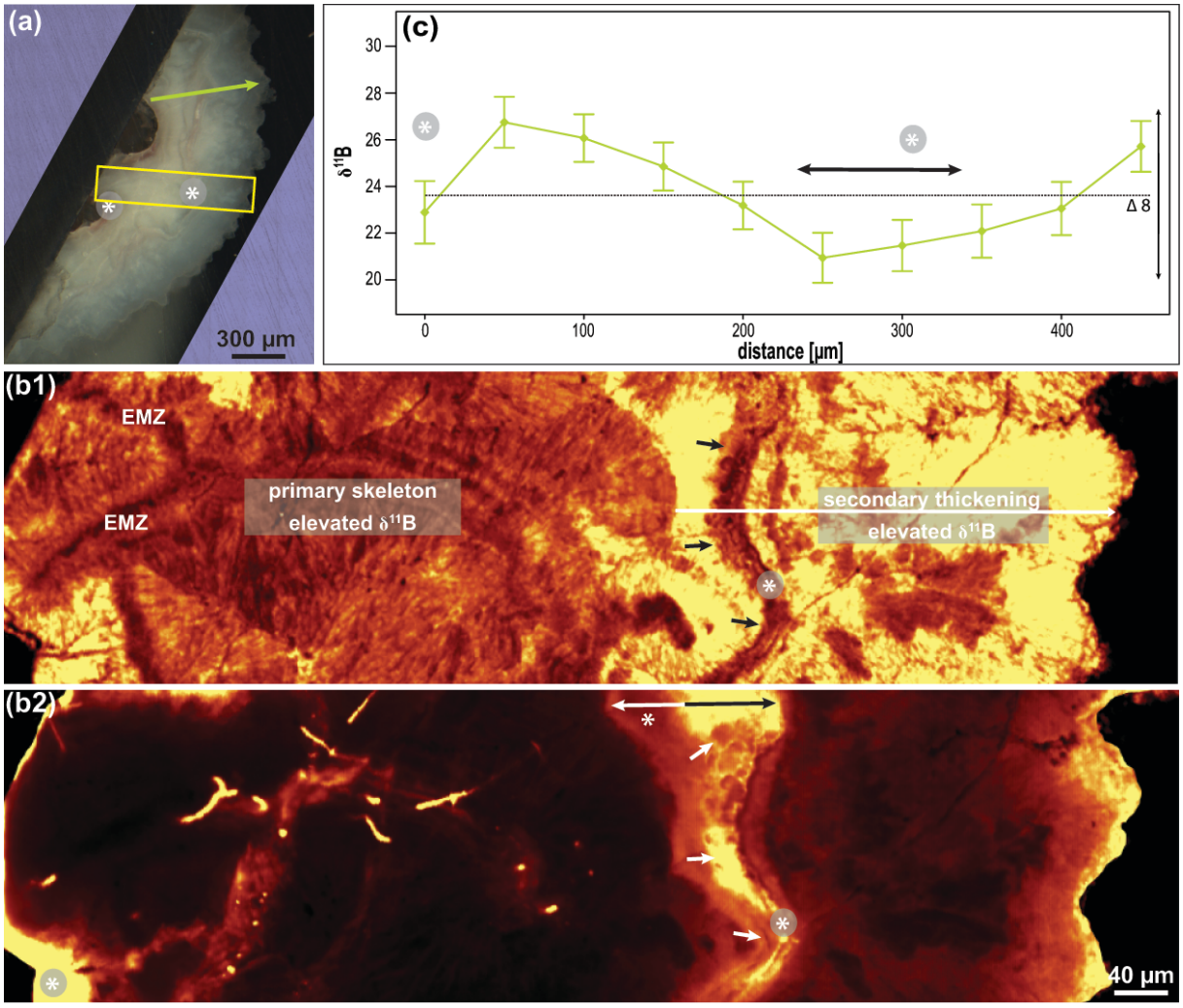

Figure S5: Young branch of *Lophelia pertusa* cut in transversal plane and prepared for Raman mapping and SIMS analysis. (a) Microscopic image contains the location of the Raman map and the SIMS transects. Red asterisks mark the location of the staining line. (b) Raman map of the intensity distribution of the main aragonite peak (symmetric stretch, 1085 cm^{-1}) reveals the early mineralization zone (EMZ), the primary skeleton and the area of secondary thickening. Arrows mark the skeletal growth interruption at the staining line. (b2) Raman fluorescence map displays the location of the staining line and difference in width. c) $\delta^{11}B$ measured from inside to the outer coral skeletal rim (transect #8)